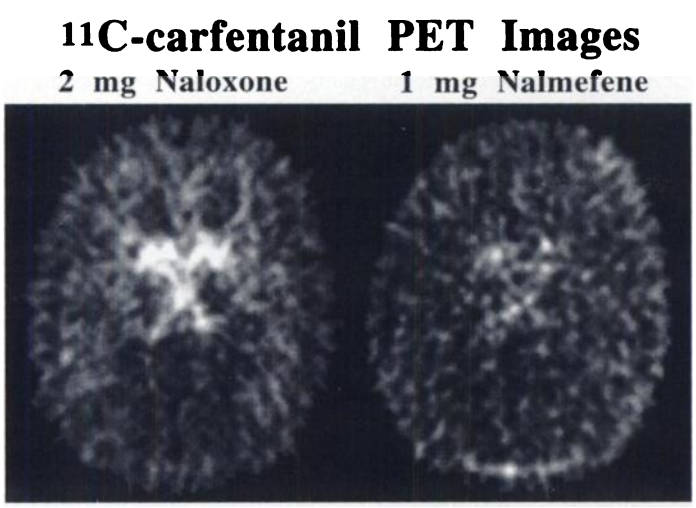

FIGURE 5. PET scans obtained 8 hr after the administration of 2 mg of naloxone (left) and 1 mg of nalmefene (right). The binding of [^{11}C]carfentanil in the striatum and thalamus after nalmefene administration is significantly less than that after naloxone administration.

ACKNOWLEDGMENTS

This study was sponsored by Ohmeda, Inc., Liberty Corner, NJ. We would like to thank Madge M. Murrell, Julia Buchanan, Robert C. Smoot, William B. Mathews, John L. Musachio, Allen B. Gardiner, Kathleen E. Truelove, Clem E. Whitman, Zsolt Szabo and Utit Pitaktong for their excellent support.

REFERENCES

1. Pasternak GW. *The Opiate Receptors*. New York, NY: Humana Press; 1988.
2. Kennedy SK, Longnecker DE. History and principles of anesthesiology. In: Goodman Gilman A, Rall TW, Nies AS, Taylor P, eds. *The pharmacological basis of therapeutics*. New York, NY: Pergamon Press; 1990:260–275.
3. Johnstone R, Jobes DR, Kennell EM, Behar MG, Smith TC. Reversal of morphine anesthesia with naloxone. *Anesthesiology* 1974;41:361–367.
4. Evans JM, Hogg MIJ, Lunn JN, Rosen M. Degree and duration of reversal by naloxone of effects of morphine in conscious subjects. *Br Med J* 1974;2:589–591.
5. Ngai SH, Berkowitz BA, Yang JC, Hempstead J, Spector S. Pharmacokinetics of naloxone in rats and in man. *Anesthesiology* 1976;44:398–401.
6. Jaffe JH, Martin WR. Opioid analgesics and antagonists. In: Goodman Gilman A, Rall TW, Nies AS, Taylor P, eds. *The pharmacological basis of therapeutics*. New York, NY: Pergamon Press; 1990:491–531.
7. Ling W, Wesson DR. Drugs of abuse: opiates. *West J Med* 1990;152:565–572.
8. Foldes FF, Lunn JN, Moore J, Brown IMN. Allylnoroxymorphone. A new potent narcotic antagonist. *Am J Med Sci* 1963;245:23–30.
9. Sadove MS, Balagot RC, Hatano S, Jobgen EA. Study of a narcotic antagonist: N-allyl-noroxymorphone. *J Am Med Assoc* 1963;183:666–668.
10. Barsan WG, Seger D, Danzl DF, et al. Duration of antagonistic effects of nalmefene and naloxone in opiate-induced sedation for emergency department procedures. *Am J Emerg Med* 1989;7:155–161.
11. Kaplan JL, Marx JA. Effectiveness and safety of intravenous nalmefene for emergency department patients with suspected narcotic overdose: a pilot study. *Ann Emerg Med* 1991;22:187–190.
12. Van Vugt DA, Webb MY, Reid RL. Comparison of the duration of action of nalmefene and naloxone on the hypothalamic-pituitary axis of the rhesus monkey. *Neuroendocrinology* 1989;49:275–280.
13. Gal TJ, DiFazio CA. Prolonged antagonism of opioid action with intravenous nalmefene in man. *Anesthesiology* 1986;64:175–180.
14. Gal TJ, DiFazio CA, Dixon R. Prolonged blockade of opioid effect with oral nalmefene. *Clin Pharmacol Ther* 1986;40:537–542.
15. Frost JJ, Wagner HN Jr, Dannals RF, et al. Imaging opiate receptors in the human brain by positron tomography. *J Comput Assist Tomogr* 1985;9:231–236.
16. Frost JJ, Mayberg HS, Sadzot B, et al. Comparison of [^{11}C]diprenorphine and [^{11}C]carfentanil binding to opiate receptors in humans by positron emission tomography. *J Cereb Blood Flow Metab* 1990;10:484–492.
17. Bice AN, Wagner HN Jr, Frost JJ, et al. A simplified detection system for neuroreceptor studies in the human brain. *J Nucl Med* 1986;27:184–191.
18. Lee MC, Wagner HN Jr, Tanada S, Frost JJ, Bice AN, Dannals RF. Duration of occupancy of opiate receptors by naltrexone. *J Nucl Med* 1988;29:1207–1211.
19. Villemagne VL, Frost JJ, Dannals RF, et al. Comparison of ^{11}C-diprenorphine and ^{11}C-carfentanil in vivo binding to opiate receptors in man using a dual detector system. *Eur J Pharmacol* 1994;257:195–197.
20. Dannals RF, Ravert HT, Frost JJ, Wilson AA, Burns HD, Wagner HN Jr. Radiosynthesis of an opiate receptor binding radiotracer: [^{11}C]carfentanil. *Int J Appl Radiat Isot* 1985;36:303–306.
21. Mayberg HS, Frost JJ. Opiate receptors. In: Frost JJ, Wagner HN Jr, eds. *Quantitative imaging*. New York, NY: Raven Press; 1990:81–95.
22. Aitkenhead AR, Derbyshire DR, Pinnock CA, Achola K, Smith G. Pharmacokinetics of intravenous naloxone in healthy volunteers [Abstract]. *Anesthesiology* 1984;61: A381.
23. Dixon R, Hsiao J, Taaffe W, Hahn E, Tuttle R. Nalmefene. Radioimmunoassay for a new opioid antagonist. *J Pharm Sci* 1984;73:1645–1646.
24. Dixon R, Howes J, Gentile J, et al. Nalmefene. Intravenous safety and kinetics of a new opioid antagonist. *Clin Pharmacol Ther* 1986;39:49–53.
25. Michel ME, Bolger G, Weissman B. Binding of a new opiate antagonist, nalmefene, to rat brain membranes. *Methods Find Exp Clin Pharmacol* 1985;7:175–177.

Metabolism of Technetium-99m-L,L-Ethyl Cysteinate Dimer in Rat and Cynomolgus Monkey Tissue

Yusuke Inoue, Toshimitsu Momose, Tohru Ohtake, Junichi Nishikawa, Yasuhito Sasaki, Takaki Waritani and Minoru Inoue
Department of Radiology, University of Tokyo, and Daiichi Radioisotope Laboratories, Ltd., Tokyo, Japan

Technetium-99m-L,L-ethyl cysteinate dimer (^{99m}Tc-ECD) is thought to be hydrolyzed in the brain by an enzyme and to be trapped as a hydrophilic product. We investigated the characteristics of the enzymatic system that metabolizes ^{99m}Tc-ECD. **Methods:** In 50 m*M* phosphate buffer (pH 7.4), ^{99m}Tc-ECD was incubated with various concentrations of homogenates of rat tissues (blood, liver and brain) or cynomolgus monkey tissues (blood, liver, cerebral gray matter, cerebral white matter and cerebellar gray matter), and the metabolic rates were assessed. Inhibition studies were performed using diisopropyl fluorophosphate, eserine and p-chloromercuribenzoate as inhibitors. The metabolic rates in the brain homogenates of rat and monkey were measured at various levels of pH, ranging from 6.6 to 7.6. Technetium-99m-L,L-ethyl cysteinate dimer metabolism was also examined in the presence of purified enzymes. **Results:** In both species, the metabolic rate was high in liver tissue, intermediate in brain tissue and low in blood. The rate in cerebral gray matter of cynomolgus monkey was higher than those in rat brain, monkey cerebral white matter and monkey cerebellar gray matter. All substances used as inhibitors depressed ^{99m}Tc-ECD metabolism, and the response was different among tissues. Reduction in pH induced slight decreases in metabolic rate. Hydrophilic conversion of ^{99m}Tc-ECD was observed after incubation with porcine liver carboxylesterase. **Conclusion:** These results support the hypothesis that the hydrophilic conversion of ^{99m}Tc-ECD is mediated by enzymes. It is also suggested that various enzymes catalyze the hydrolysis of ^{99m}Tc-ECD and that the enzymatic system that metabolizes ^{99m}Tc-ECD is different between tissues and between species.

Key Words: technetium-99m-ECD; metabolism; in vitro

J Nucl Med 1997; 38:1733–1737

Received Jul. 8, 1996; revision accepted Jan. 28, 1997.
For correspondence or reprints contact: Yusuke Inoue, MD, Department of Radiology, University of Tokyo, 7-3-1 Hongo, Bunkyo-ku, Tokyo 113, Japan.

Technetium-99m-L,L-ethyl cysteinate dimer (^{99m}Tc-ECD), a brain perfusion agent for SPECT, is widely used in various clinical situations (*1*). After its intravenous injection, ^{99m}Tc-

ECD is taken up by the brain in a distribution pattern approximately consistent with regional cerebral blood flow and is retained for a relatively long period. In contrast, radioactivity is removed rapidly from the blood. This radiotracer is an excellent brain perfusion agent, is stable in the brain and has rapid blood clearance (*2*).

Enzymatic trapping is considered to be the mechanism by which radioactive materials are retained in the brain after ^{99m}Tc-ECD administration (*3–5*). This radiotracer is lipophilic and crosses the blood–brain barrier. It is hydrolyzed to ^{99m}Tc-ethyl cysteinate monomer in the brain by an unknown enzyme. The metabolite is hydrophilic and does not permeate the blood–brain barrier; thus, "trapping" of radioactive material occurs. The enzymatic process is also thought to be related to the rapid clearance of ^{99m}Tc-ECD from the bloodstream (*3,4*).

Esterase is a candidate for the enzyme that catalyzes the hydrolysis of ^{99m}Tc-ECD because the reaction that produces ^{99m}Tc-ethyl cysteinate monomer is deesterification. Esterases can be divided into three major classes: arylesterases, cholinesterases and carboxylesterases, with many enzymes in each class. Little is known about the enzyme involved in ^{99m}Tc-ECD metabolism. We evaluated the metabolism of ^{99m}Tc-ECD in the presence of tissue homogenates of rat and cynomolgus monkey. The aim of this study was to investigate the characteristics of the enzyme that catalyzes the hydrolysis of ^{99m}Tc-ECD.

MATERIALS AND METHODS

Radiopharmaceutical Preparation

We prepared ^{99m}Tc-ECD using a commercial two-vial kit. Vial A contained 0.755 μmol of ECD ligand, and vial B contained 1 ml of phosphate buffer. Saline (3 ml) was placed into vial A, and 1 ml of the solution in vial A was transferred to vial B, along with 111 MBq of fresh sodium ^{99m}Tc-pertechnetate solution in a volume of 1 ml. Sodium ^{99m}Tc-pertechnetate solution was obtained from a commercial ^{99}Mo/^{99m}Tc generator, from which the previous elution had been performed about 3 hr before. The solution in vial B was allowed to stand at room temperature for at least 30 min, and labeled ECD was thus prepared. The concentration of the ECD ligand was 252 μ*M* in the final solution, and the concentration of radioactivity was about 37 MBq/ml.

Estimation of Lipophilic Content

The radiochemical purity (RCP) of ^{99m}Tc-ECD solution was determined by thin-layer chromatography (TLC) on silica gel TLC plates, using ethyl acetate as a solvent. A solution with a RCP of >95% was used in the experiments.

The residual lipophilic content after the incubation of ^{99m}Tc-ECD with animal tissue was also assessed by the same TLC. From the tube containing the solution with radioactive material and animal tissue, 0.5 ml of solution was transferred into the iced tube with 2.5 ml of ethanol. After vortex mixing, the tube was centrifuged at 1500 × *g* for 10 min, and an aliquot of the supernatant was analyzed by TLC. The radioactivity in the precipitated portion was less than 1% of the radioactivity in the centrifuged tube and was ignored in the analysis. The ratio of the unmetabolized parent (R_p) was determined as the ratio of the radioactivity of $R_f > 0.4$ to overall radioactivity. The ratio of metabolites (R_m) was obtained from RCP and the parent ratio as follows: R_m (%) = [(RCP − R_p)/RCP] × 100.

Effect of Unlabeled ECD

The metabolic rate of ^{99m}Tc-ECD was estimated in the presence of various amounts of unlabeled ECD, and the effect of unlabeled ECD on ^{99m}Tc-ECD metabolism was evaluated.

Unlabeled ECD was added to ^{99m}Tc-ECD solution, prepared as described above, and a series of solutions with a particular concentration of ^{99m}Tc-ECD and various concentrations of unlabeled ECD were produced. These solutions were transferred into tubes containing tissue homogenates in 50 m*M* phosphate buffer (pH 7.4) and were incubated at 37°C. The tissues used in this study were rat blood (final concentration, 0.072 ml/ml), rat liver (0.0006 g/ml) and rat brain (0.006 g/ml). Assuming that the amount of ^{99m}Tc-ECD and ^{99}Tc-ECD was negligible, the final concentration of unlabeled ECD ranged from 2.52 μ*M* to 570.2 μ*M*. From the tube, 0.5 ml of the solution was sampled 5, 10, 15, 20, 25 and 30 min after the start of incubation, and the ratio of metabolites in the sample was assessed by TLC. The ratio was plotted against incubation time, and linear regression analysis was performed by the least squares method. The ratio of metabolites at time 0 was set at 0. The metabolic rate (%/min) was defined as the slope of the regression line. Ratios of metabolites above 15% were not used in the analysis to assess the initial rate of reaction precisely. As controls, ^{99m}Tc-ECD solutions with various concentrations of ECD were placed into tubes containing 50 m*M* phosphate buffer without animal tissue. They were incubated for 30 min, and the lipophilic content was assessed after the incubation.

Metabolic Rate in Rat and Monkey Tissues

The metabolic rates of ^{99m}Tc-ECD in the tissues of rat and cynomolgus monkey were estimated based on the initial rate of reaction study.

In 50 m*M* phosphate buffer (pH 7.4), ^{99m}Tc-ECD solution was mixed with various concentrations of tissue homogenates and incubated at 37°C. The tissues examined included rat blood (final concentration, 0.025–0.15 ml/ml), rat liver (0.00025–0.002 g/ml), rat brain (0.003–0.015 g/ml), monkey blood (0.01–0.08 ml/ml), monkey liver (0.0003–0.002 g/ml), monkey cerebral gray matter (0.0002–0.0024 g/ml), monkey cerebral white matter (0.001–0.008 g/ml) and monkey cerebellar gray matter (0.002–0.01 g/ml). The final concentration of the ligand was 25.2 μ*M*. From the tube, 0.5 ml of solution was sampled 5, 10, 15, 20, 25 and 30 min after the start of incubation, and the ratio of metabolites was assessed by TLC. The metabolic rate (%/min) was obtained by the method described above. The relationship between the metabolic rate and concentration of tissue was examined by linear regression analysis.

Inhibition Studies

Rat or cynomolgus monkey tissue and ^{99m}Tc-ECD were incubated in the presence of esterase inhibitors, and the inhibitory effects were investigated.

In 50 m*M* phosphate buffer (pH 7.4), with and without an inhibitor, ^{99m}Tc-ECD was mixed with tissue homogenates and incubated at 37°C for 30 min. The tissues examined in this study were rat blood (final concentration, 0.09 ml/ml), rat liver (0.0008 g/ml), rat brain (0.007 g/ml), monkey blood (0.14 ml/ml), monkey liver (0.0009 g/ml) and monkey cerebral gray matter (0.003 g/ml). Diisopropyl fluorophosphate (DFP; 500 μ*M* and 100 μ*M*), eserine (10 μ*M*) and p-chloromercuribenzoate (PCMB; 5 m*M* and 1 m*M*) were used as inhibitors. These substances are known to have an inhibitory effect on esterase-mediated reactions (*6*). The final concentration of ECD ligand was 25.2 μ*M*. The experiments were performed in triplicate. After incubation, 0.5 ml of solution was sampled, and the ratio of metabolites was assessed by TLC. The ratio of metabolites with an inhibitor was compared with that without an inhibitor, and the presence of an inhibitory effect was determined. In addition, ^{99m}Tc-ECD and inhibitors were incubated in 50 m*M* phosphate buffer at 37°C for 30 min without animal tissue, and the radiochemical stability of ^{99m}Tc-ECD in the presence of the inhibitors was examined.

pH Dependence

The effect of pH on ^{99m}Tc-ECD metabolism in brain homogenates of rat and cynomolgus monkey was examined.

The solution with ^{99m}Tc-ECD was placed into a tube containing homogenates of rat brain (final concentration, 0.0063 g/ml) or monkey brain (0.0022 g/ml) in 50 m*M* phosphate buffer and incubated at 37°C for 30 min. The phosphate buffer ranged in pH from 6.6 to 7.6. The final concentration of ECD ligand was 25.2 μM. After incubation, 0.5 ml of solution was sampled, and the ratio of metabolites was assessed by TLC. In addition, incubation was performed in the absence of brain homogenates, and the stability of ^{99m}Tc-ECD was evaluated at various levels of pH.

Metabolism by Purified Enzyme

It was also investigated whether purified or recombinant esterase catalyzes the hydrolysis of ^{99m}Tc-ECD. The esterases examined were porcine liver carboxylesterase, human recombinant acetyl cholinesterase and horse serum butyl cholinesterase. Esterase (final concentration, 10 units/ml) and ^{99m}Tc-ECD were incubated in 50 m*M* phosphate buffer (pH 7.4) at 37°C for 30 min. After incubation, the ratio of metabolites was determined by TLC. The experiments were performed in triplicate.

RESULTS

Effect of Unlabeled ECD

Incubation without animal tissue did not change the RCP, indicating the radiochemical stability of ^{99m}Tc-ECD under the conditions provided in this study. The ratio of metabolites was below 15% in every sample, and all seven points were used in the linear regression in each experiment. The metabolic rate in rat liver was reduced as the concentration of unlabeled ECD increased, indicating an inhibitory effect of unlabeled ECD on ^{99m}Tc-ECD metabolism, and the rate at 570.2 μM was 44% of that at 2.52 μM (Fig. 1). In rat blood and rat brain, the metabolic rate was almost constant, irrespective of the concentration of unlabeled ECD, and no substantial effect of unlabeled ECD was observed.

Metabolic Rate in Rat and Monkey Tissues

Only three points each were used in the linear regression in four experiments (0.15 ml/ml rat blood, 0.002 g/ml rat liver, 0.015 ml/ml rat brain and 0.002 g/ml monkey liver) because ratios of metabolites were above 15% in four samples. In the other experiments, four to seven points were used to determine the metabolic rate (Fig. 2). There was a high positive correlation between metabolic rate and the concentration of animal tissue (Fig. 3). The y-intercept of the obtained regression line was close to 0, and the metabolic rate was almost proportional to the concentration of animal tissue. Corrected metabolic rate was defined as metabolic rate (%/min) divided by the concentration of animal tissue (ml/ml in blood and g/ml in the other tissues), and the mean of the corrected metabolic rates in various concentrations of each tissue was calculated (Table 1). In both rat and cynomolgus monkey, the corrected metabolic rate was low in blood and high in liver. The rates in intracranial tissues were between those in blood and liver. The rate in cerebral gray matter of cynomolgus monkey was higher than those in rat brain, monkey cerebral white matter and monkey cerebellar gray matter.

Inhibition Studies

After the incubation of ^{99m}Tc-ECD with inhibitors and without animal tissue, RCP was unchanged, and ^{99m}Tc-ECD was found to remain stable. The results of inhibition studies are presented in Figure 4. The reaction in rat blood, rat liver, monkey liver and monkey cerebral gray matter was depressed by DFP. The rate of hydrolysis in rat liver was reduced in the presence of eserine. Metabolism in tissues other than rat blood was depressed by PCMB.

pH Dependence

The radiochemical stability of ^{99m}Tc-ECD was confirmed in the range of pH examined. The metabolic rate was slightly reduced in brain homogenates of both species as pH decreased (Fig. 5).

Metabolism by Purified Enzyme

In the presence of porcine liver carboxylesterase, 80.8% of ^{99m}Tc-ECD was hydrolyzed in 30 min, whereas no substantial ratio of metabolites was observed in the solution incubated with human recombinant acetyl cholinesterase or horse serum butyl cholinesterase.

DISCUSSION

Cerebral accumulation of ^{99m}Tc-ECD is thought to depend on enzymatic trapping (*3–5*), and changes in metabolic activity may cause changes in retention of the tracer. An understanding of the enzymatic system seems to be important for the clinical application and interpretation of SPECT using this radiopharmaceutical. The results of this study support the hypothesis that the metabolism of ^{99m}Tc-ECD is mediated by esterase. Some characteristics of the enzymatic process were also elicited.

Effect of Unlabeled ECD

Technetium-99m-L,L-ethyl cysteinate dimer solution contains ^{99}Tc-ECD and unlabeled ECD. The ligand labeled with ^{99}Tc is considered to have the same chemical characteristics as ^{99m}Tc-ECD and to cause competitive inhibition of the enzyme that metabolizes ^{99m}Tc-ECD. Unlabeled ECD may also be assumed to have an inhibitory effect on ^{99m}Tc-ECD metabolism. In the study with various concentrations of unlabeled ECD, this effect was not observed in rat blood or rat brain. Although an inhibitory effect was indicated in rat liver, it seems to be small unless the concentration of unlabeled ECD is high. The metabolic rate in the presence of 570.2 μM ECD is still about half of the rate with 2.52 μM ECD. It should be noted that a commercial kit contains only 0.755 μmol of ECD ligand. Other studies, including determination of metabolic rate in various tissues and inhibition studies, were performed with 25.2 μM ECD ligand, and the inhibitory effect of unlabeled ECD appears to be limited. ECD is a relatively small molecule. The coordination of ^{99m}Tc may substantially change its stereostructure and, consequently, its affinity to enzymes. The observation in this study suggests that the presence of unlabeled ECD is not a serious problem in investigating ^{99m}Tc-ECD metabolism. However, because only rat tissues were examined, a larger effect of unlabeled ECD cannot be excluded in monkey tissues.

Metabolic Rate in Rat and Monkey Tissues

Because excessive reaction causes underestimation of the reaction rate in an initial rate of reaction study, ratios of metabolites above 15% were excluded in the linear regression analysis. In four experiments, only three points were used in the analysis, and this appears to impair the reliability of the results of these experiments. In other experiments, four or more points were used.

The metabolic rate in tissue homogenates of rat and cynomolgus monkey was proportional to the concentration of each tissue, indicating that the reaction is a first-order reaction to the tissue concentration. This is consistent with the hypothesis that

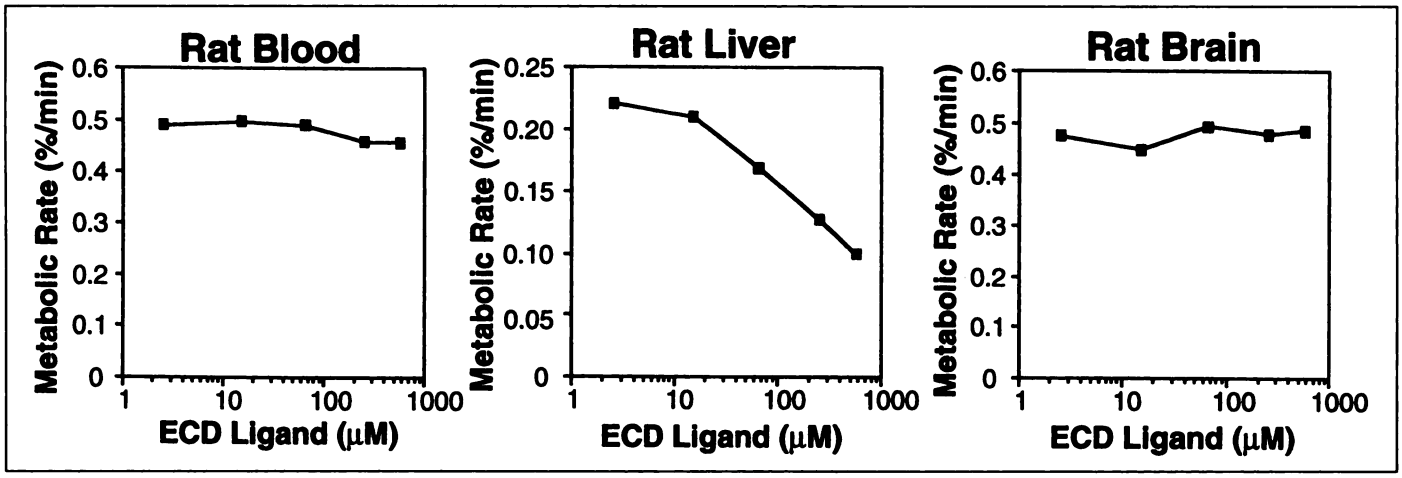

FIGURE 1. Effect of unlabeled ECD on ^{99m}Tc-ECD metabolism in homogenates of rat blood and tissues.

the hydrophilic conversion of ^{99m}Tc-ECD depends on a substance in the tissue.

The metabolic rate was first calculated as the amount (in mole) of the parent compound metabolized per minute and expressed as a percentage of the initial amount of the parent, then corrected for tissue concentration. The corrected metabolic rate was expressed as %/min/(g/ml) or %/min/(ml/ml). Insofar as the concentration of labeled ECD is low, the metabolic rate in the unit of mole/min/(g/ml) is assumed to be proportional to the ^{99m}Tc-ECD concentration. The rate expressed in the unit of %/min/(g/ml) should be constant, irrespective of the ^{99m}Tc-ECD concentration, and thus the rate is considered to be an index of metabolic activity in the tissue. This does not hold true when the metabolic rate is measured in a solution with a high concentration of substrate compared with the Michaelis–Menten constant of the enzyme. Walovitch et al. (*5*) reported a Michaelis–Menten constant of 11.05 μM in brain tissue of rhesus monkey. We prepared ^{99m}Tc-ECD using the kit and a small amount of ^{99m}Tc-pertechnetate. Although the solution incubated in our experiments had a high total concentration of labeled and unlabeled ECD relative to the reported Michaelis–Menten constant, it is considered to have contained only a trace amount of labeled ECD. Although the presence of unlabeled ECD may have interfered with the reaction, the inhibitory effect of unlabeled ECD was considered to be small. The metabolic rate obtained in this study appears to approximately represent the metabolic activity in the tissue.

In cynomolgus monkey the metabolic rate in cerebral gray matter was higher than those in cerebral white matter and cerebellar gray matter. It has been proposed that metabolic activity is higher in baboon brain than in baboon cerebellum (*7*), although no comparison between gray and white matter was made. The metabolic activity in the brain may influence the efficiency of retention in the brain and, consequently, in SPECT images using ^{99m}Tc-ECD. High metabolic activity in cerebral gray matter could make the contrast between gray and white matter higher. Different kinetics between gray and white matter have been shown for ^{123}I-labeled isopropyl iodoamphetamine (*8*), and there may be such a difference for ^{99m}Tc-ECD. The difference between cerebral and cerebellar gray matter may reduce cerebellar accumulation relative to cerebral accumulation. High accumulation in the medial aspect of the occipital lobe is reported in normal human subjects who have their eyes closed (*9*). This may be attributable to regional differences in metabolic activity in the human brain. It has not been determined whether the differences in metabolic activity actually cause differences in the efficiency of brain retention. The relation between regional metabolic activity and brain SPECT images using ^{99m}Tc-ECD remains to be investigated.

Rat brain was not divided into gray and white matter. Although this makes detailed comparison between rat brain and monkey brain difficult, metabolic activity in rat brain seems to be lower than that in monkey brain. Low metabolic activity may explain, at least in part, the poor retention of ^{99m}Tc-ECD in rat brain (*5*). In both species, metabolic activity in liver was high, and activity in blood was low. The liver may play an important role in extracranial metabolism to excrete the radioactive material, although other organs such as kidney and lung may also act as metabolic organs (*7,10*).

Inhibition Studies

Substances that are known to inhibit esterase had an inhibitory effect on the hydrolysis of ^{99m}Tc-ECD, consistent with the

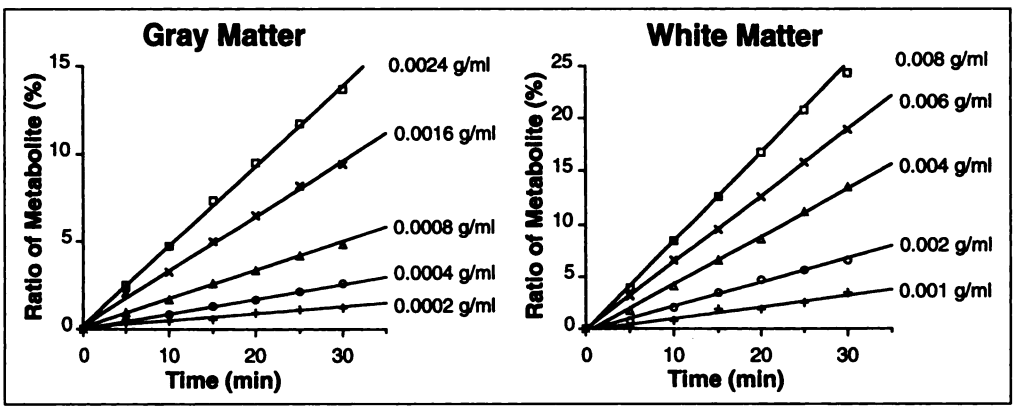

FIGURE 2. Temporal profiles of the ratios of metabolites in incubations with homogenates of cerebral gray matter and cerebral white matter of cynomolgus monkey. Data at 20–30 min in 0.008 g/ml white matter and data at 25 and 30 min in 0.006 g/ml white matter were not used in the analysis. The curves represent regression lines.

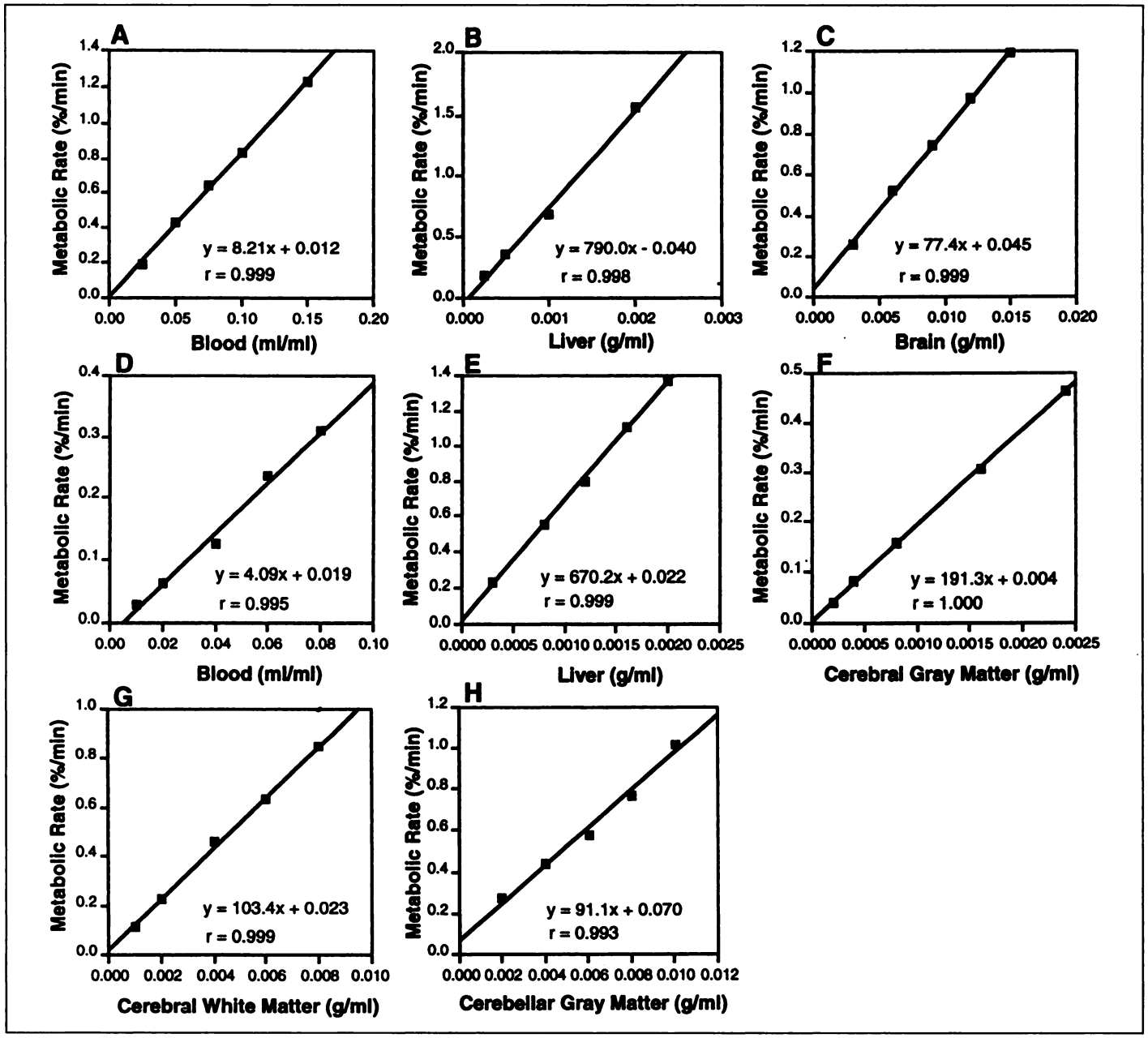

FIGURE 3. Relationship between metabolic rate and concentration of tissue homogenates of rat and cynomolgus monkey. (A–C) Rat tissues. (D–H) Cynomolgus monkey tissues.

TABLE 1
Metabolic Rate Corrected for Concentration of Animal Tissue

Species	Tissue	Metabolic rate [%/min/(g/ml)]*
Rat	Blood	8.3 ± 0.3
	Liver	790.0 ± 38.0
	Brain	83.6 ± 3.3
Cynomolgus monkey	Blood	3.6 ± 0.5
	Liver	703.4 ± 47.2
	Cerebral gray matter	205.9 ± 5.4
	Cerebral white matter	111.2 ± 5.0
	Cerebellar gray matter	108.5 ± 17.7

Values are presented as mean ± s.d.
*%/min/(ml/ml) in blood.

hypothesis that its metabolism is catalyzed by esterase. In some experiments, the ratio of metabolites exceeded 15%, which was the upper limit to include in the analysis in the metabolic rate study. This may impair the proportionality between true metabolic activity and observed ratio of metabolites; however, it does not seem to be a substantial problem in investigating whether the inhibitory effect is present or not.

Inhibitory response differed among the tissues. Carboxylesterase is inhibited by DFP, cholinesterase is inhibited by DFP and eserine and arylesterase is inhibited by PCMB (*6*). Based on the results of the inhibition studies, it is supposed that the enzymes that mainly catalyze the hydrolysis of ^{99m}Tc-ECD are arylesterase in rat brain and monkey blood and carboxylesterase in rat blood. Both arylesterase and carboxylesterase are thought to act in monkey liver and monkey cerebral gray matter. In rat

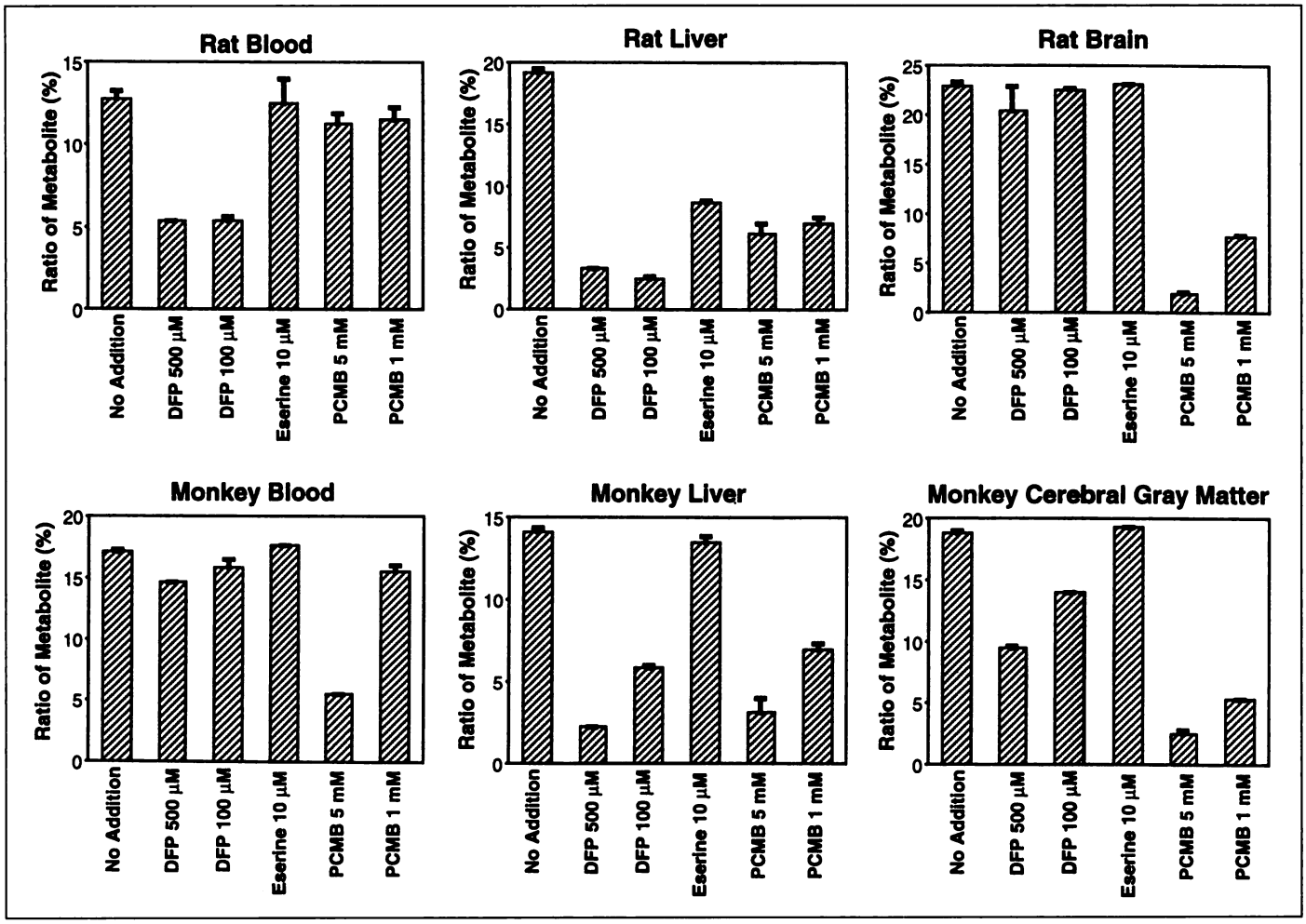

FIGURE 4. Results of inhibition studies in rat and cynomolgus monkey. No Addition = incubation with no inhibitor.

liver, arylesterase and cholinesterase are thought to mediate ^{99m}Tc-ECD metabolism, although carboxylesterase may also be involved.

Various enzymes catalyze the hydrolysis of ^{99m}Tc-ECD, and the enzymatic systems are different between tissues and between species. In investigating the metabolism of ^{99m}Tc-ECD, attention should be paid to the quantitative and qualitative differences in the enzyme among tissues.

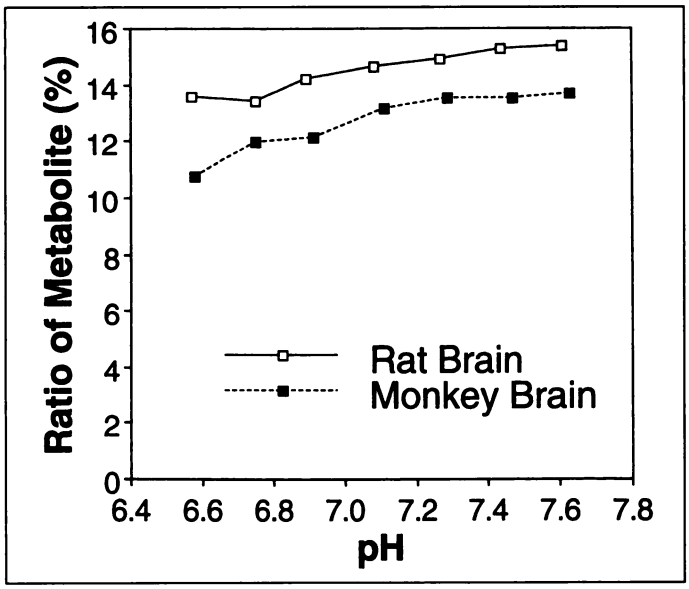

FIGURE 5. Effect of pH on ^{99m}Tc-ECD metabolism in brain homogenates of rat and cynomolgus monkey.

pH Dependence

Considering that the brain retention of ^{99m}Tc-ECD depends on the enzyme, we studied the pH dependence of the enzyme in the clinical range of pH. A slight decrease in metabolic rate was observed in rat and monkey brain at a low level of pH. The change in metabolic rate was small, however, compared with the regional difference in monkey brain. The effect of pH on ^{99m}Tc-ECD metabolism does not seem to create serious problems in SPECT imaging using this radiopharmaceutical.

Metabolism by Purified Enzyme

Walovitch et al. (*4*) reported that neither acetyl cholinesterase nor butyl cholinesterase mediates the metabolism of ^{99m}Tc-ECD. This was confirmed by our experiment. On the other hand, the radiopharmaceutical was hydrolyzed when incubated with porcine liver carboxylesterase, confirming that the metabolism of ^{99m}Tc-ECD can be catalyzed by esterase.

Technetium-99m-L,L-ethyl cysteinate dimer metabolism is mediated by an enzyme, which is probably esterase. Arylesterase, carboxylesterase and cholinesterase may be involved in the reaction, and different enzymes may play main roles in different tissues. Catalytic activity has a wide range among tissues and may vary even within the intracranial regions.

Incubation of ^{99m}Tc-ECD with tissue homogenates does not yield detailed properties of the enzymes, and protein resolution would aid in further investigation.

CONCLUSION

These studies suggest:

1. Various enzymes catalyze the hydrolysis of ^{99m}Tc-ECD, and the enzymatic systems are different between tissues and between species.
2. pH has little effect on ^{99m}Tc-ECD metabolism in the brain.
3. There are regional differences in intracranial metabolic activity in cynomolgus monkey.
4. In both rat and cynomolgus monkey tissue, metabolic activity is low in blood, intermediate in brain and high in liver.

It remains to be determined whether regional differences in metabolic activity in the intracranial tissues influence ^{99m}Tc-ECD SPECT images.

REFERENCES

1. Moretti JL, Caglar M, Weinmann P. Cerebral perfusion imaging tracers for SPECT: which one to choose? *J Nucl Med* 1995;36:359–363.
2. Leveille J, Demonceau G, De Roo M, et al. Characterization of technetium-99m-L,L-ECD for brain perfusion imaging, part 2: biodistribution and brain imaging in humans. *J Nucl Med* 1989;30:1902–1920.
3. Walovitch RC, Hill TC, Garrity ST, et al. Characterization of technetium-99m-L,L-ECD for brain perfusion imaging, part 1: pharmacology of technetium-99m ECD in nonhuman primates. *J Nucl Med* 1989;30:1892–1901.
4. Walovitch RC, Franceschi M, Picard M, et al. Metabolism of ^{99m}Tc-L,L-ethyl cysteinate dimer in healthy volunteers. *Neuropharmacology* 1991;30:283–292.
5. Walovitch RC, Cheesman EH, Maheu LJ, Hall KM. Studies of the retention mechanism of the brain perfusion imaging agent, ^{99m}Tc-bicisate (^{99m}Tc-ECD). *J Cereb Blood Flow Metab* 1994;14(suppl 1):S4–S11.
6. Holmes RS, Masters CJ. The developmental multiplicity and isoenzyme status of cavian esterases. *Biochem Biophys Acta* 1967;132:379–399.
7. Bormans G, Van Nerom C, De Beukelaer C, Hoogmartens M, De Roo M, Verbruggen A. Comparison of ^{99m}Tc-ECD metabolism in organ homogenates of rat and baboon [Abstract]. *Eur J Nucl Med* 1989;15:423.
8. Yonekura Y, Nishizawa S, Mukai T, et al. Functional mapping of flow and back-diffusion rate of N-isopropyl-p-iodoamphetamine in human brain. *J Nucl Med* 1993;34:839–844.
9. Kawashima R, Koyama M, Ito H, et al. Normal cerebral perfusion of ^{99m}Tc-ECD brain SPECT: evaluation by an anatomical standardization technique. *Kakuigaku* 1996;33: 69–72.
10. Van Nerom C, Bormans G, De Beukelaer C, De Roo M, Verbruggen A. Metabolism of ^{99m}Tc-ECD in organ homogenates of baboon [Abstract]. *Eur J Nucl Med* 1989;15:423.

Imaging Nicotinic Acetylcholine Receptors with Fluorine-18-FPH, an Epibatidine Analog

Victor L. Villemagne, Andrew Horti, Ursula Scheffel, Hayden T. Ravert, Paige Finley, David J. Clough, Edythe D. London, Henry N. Wagner, Jr. and Robert F. Dannals

Divisions of Nuclear Medicine and Radiation Health Sciences, The Johns Hopkins Medical Institutions; and Brain Imaging Section, Intramural Research Program, National Institute on Drug Abuse, National Institutes of Health, Baltimore, Maryland

Nicotinic acetylcholine receptors (nAChRs) have been implicated in a variety of central processes, such as learning and memory and analgesia. These receptors also mediate the reinforcing properties of nicotine in tobacco products and are increased in postmortem samples of brains of smokers. On the other hand, brains of individuals who have died from dementia of the Alzheimer type show abnormally low densities of nAChRs. In this study, the distribution and kinetics of [(±)-exo-2-(2-[^{18}F] fluoro-5-pyridyl)-7-azabicyclo[2.2.1]heptane (^{18}F-FPH), a high-affinity nAChR agonist, was evaluated in a baboon using PET. **Methods:** After intravenous injection of 5 mCi [185 MBq] ^{18}F-FPH into a 25-kg anesthetized baboon, sequential quantitative tomographic data were acquired over a period of 150 min. Regions of interest were placed and time-activity curves were generated. Brain kinetics of the radiotracer were calculated, and the in vivo regional binding in the baboon brain was compared with the known in vitro regional distribution of nAChRs in the rat and human brain. **Results:** Brain activity reached a plateau within 60 min after injection of the tracer, and the binding was reversible. Elimination of ^{18}F-FPH was relatively rapid from the cerebellum (clearance $t_{1/2}$ = 3 hr), intermediate from the hypothalamus/midbrain ($t_{1/2}$ = 7 hr) and slow from the thalamus ($t_{1/2}$ = 16 hr). Radioactivity due to ^{18}F-FPH at 130 min postinjection was highest in the thalamus and hypothalamus/midbrain, intermediate in the neocortex and hippocampus and lowest in the cerebellum. Subcutaneous injection of 1 mg/kg cytisine 45 min after injection of the radiotracer reduced brain activity at 130 min by 67%, 64%, 56% and 52% of control values in the thalamus, hypothalamus/midbrain, hippocampus and cerebellum, respectively. The regional binding of ^{18}F-FPH at 130 min was highly correlated with the known densities of nAChR measured in vitro in human (r = 0.81) and rat brain (r = 0.90). **Conclusion:** These results demonstrate the feasibility of imaging nAChRs in vivo. Fluorine-18-FPH appears to be a suitable tracer to study nAChRs in the human brain.

Key Words: nicotinic receptors; PET; nonhuman primate; brain; epibatidine

J Nucl Med 1997; 38:1737–1741

Nicotinic acetylcholine receptors (nAChRs) have been implicated in a variety of central processes, such as learning and memory (*1–4*) and antinociception (*5*). These receptors also mediate the reinforcing properties of nicotine in tobacco products (*6,7*). The loss of cholinergic neurons in the basal forebrain has been associated with a variety of pathological disorders, such as senile dementia of the Alzheimer type, Huntington's and Parkinson's diseases and progressive supranuclear palsy (*8–15*).

Neuronal nAChRs are ligand-gated ion channels composed of two kinds of subunits (α and β) (*1*). There are at least three subtypes of nAChRs in the central nervous system as identified by radioligand binding techniques (*1,16*): (a) those with high affinity for (-)-nicotine, which are labeled by agonists such as ^{3}H-acetylcholine and ^{3}H-cytisine (nicotine/ACh) (*17*); (b) those with high affinity for ^{125}I-α-bungarotoxin (αBgT) (*18*); and (c) those that selectively recognize neuronal bungarotoxin (n-BgT) (*19*). The pharmacological profile of a receptor subtype is related to its subunit combination. There is a good correlation between the distribution of nAChRs with the $\alpha4\beta2$ subunit combination and the distribution of high-affinity nicotine/ACh

Received Sep. 12, 1996; revision accepted Dec. 19, 1996.

For correspondence or reprints contact: Robert F. Dannals, PhD, Division of Nuclear Medicine, The Johns Hopkins Medical Institutions, 615 North Wolfe St., Room 2001, Baltimore, MD 21205–2179.